Available online at www.sciencedirect.com
ScienceDirect
Journal of the European Ceramic Society 27 (2007) 3011–3016
www.elsevier.com/locate/jeurceramsoc

Upper limit of x in $Ba_{6-3x}Nd_{8+2x}Ti_{18}O_{54}$ new tungsten bronze solid solution

L. Zhang, X.M. Chen *, N. Qin, X.Q. Liu

Department of Materials Science and Engineering, Zhejiang University, Hangzhou 310027, China

Available online 21 March 2007

Abstract

In the present work, the upper limit of x in $Ba_{6-3x}Nd_{8+2x}Ti_{18}O_{54}$ ceramics was determined by investigating the phase constitution as the function of composition and process conditions. For the compositions of $x \leq 0.75$, the new tungsten bronze structure is stable and the single phase structure is easy to be obtained. While, the new tungsten bronze structure becomes unstable for compositions of $x = 0.8$, 0.9 and 1.0, where the new tungsten bronze major phase is generally detected together with some secondary phases. The excellent microwave dielectric characteristics are not only obtained at $x = 0.67$ but also obtained at 0.8 and 0.9.

Keywords: Powders-solid state reaction; X-ray methods; Dielectric properties; Functional applications; Microwave dielectric ceramics

1. Introduction

Ceramics with compositions in the vicinity of $BaLn_2Ti_4O_{12}$ (Ln: rare earth) solid solution in the $BaO–Ln_2O_3–TiO_2$ system have attracted much scientific and commercial interests as important high-ε microwave dielectric materials.[1–12] Bolton[1] first investigated the $BaO–Ln_2O_3–TiO_2$ system, and about 10 years later, Kolar et al.[2,3] reported the ternary phases $BaNd_2Ti_3O_{10}$ and $BaNd_2Ti_5O_{14}$, which have a temperature-stable high dielectric constant, ε, and low dielectric loss. At almost the same time, Razogon et al.[4] reported the compound $BaNd_2Ti_4O_{12}$, and another compound, $Ba_{3.75}Pr_{9.5}Ti_{18}O_{54}$, was reported by Matveeva et al.[5] Since then, several groups have investigated the microwave dielectric properties and the modification of ceramics in the $BaO–Nd_2O_3–TiO_2$ system,[6–22] and many efforts also have been made to deal with the crystal-chemistry issues in the present system.[6,7,10,11] Now, the most acceptable formula for the solid solution phase with a TiO_2-rich composition in the $BaO–Ln_2O_3–TiO_2$ system is $Ba_{6-3x}Ln_{8+2x}Ti_{18}O_{54}$, but the range of x is still questionable.[6–12] The extent of solubility x is reduced with decreasing lanthanon ionic radii.[9,11] For the largest La-containing analogue, the solid solution extends from $x = 0$ to 1, while for Nd and Sm analogues, several different range of x have been reported by different groups.[6,7]

In the present paper, the upper limit of x in $Ba_{6-3x}Nd_{8+2x}Ti_{18}O_{54}$ is determined by the means of XRD analysis, and the effects of process conditions upon the phase constitution are also discussed. Moreover, the special attention is paid upon the microwave dielectric characteristics for the compositions out of the upper limit.

2. Experimental procedure

$Ba_{6-3x}Nd_{8+2x}Ti_{18}O_{54}$ ($x = 0.5$, 0.67, 0.75, 0.8, 0.9 and 1.0) ceramics were prepared by a solid-state reaction process where reagent-grade $BaCO_3$ (99.93%), Nd_2O_3 (99.9%) and TiO_2 (99.5%) powders were adopted as the raw materials. The weighed raw materials were mixed by ball milling with zirconia media in distilled water for 24 h, and the mixtures were heated at 1200 °C in air for 3 h after drying. The calcined powders, with 6 wt% of PVA added, were pressed into disks measuring 12 mm in diameter and 2–6 mm high and then sintered at 1350 °C in air for 3 h. After cooling from the sintering temperature to 1100 °C at a rate of 1 °C/min, the ceramics were naturally cooled inside the furnace. To investigate the effects of dynamic conditions upon the solid solution limit, some of the ceramics with $x = 0.75$, 0.8, 0.9 and 1.0 were quenched from the sintering temperature.

* Corresponding author. Tel.: +86 571 8795 2112; fax: +86 571 8795 2112.
E-mail address: xmchen@cmsce.zju.edu.cn (X.M. Chen).

0955-2219/$ – see front matter © 2007 Elsevier Ltd. All rights reserved.
doi:10.1016/j.jeurceramsoc.2007.01.007

The crystal phases of the calcined powders and the sintered ceramics after crushing and grinding were determined by powder X-ray diffraction (XRD) analysis, using Cu Kα radiation. The XRD data for Rietveld analysis were collected over the range of $2\theta = 10$–130° with a step size of 0.02° and a count time of 2 s. The FULLPROF program was used for Rietveld structural refinement[23]. Microwave dielectric characteristics were evaluated at 4–5 GHz using the resonator method of Hakki and Coleman.[24] Because Q factor generally varies inversely with the frequency in the microwave region, the product of Qf was used to evaluate the dielectric loss instead of Q.

3. Results and discussion

The powders calcined at 1200 °C in air for 3 h indicate the $Ba_{6-3x}Nd_{8+2x}Ti_{18}O_{54}$ tungsten bronze structure in the entire composition range of $x = 0.5$–1.0, however, minor amount of $Ba_4Ti_{13}O_{30}$ and $Nd_2Ti_2O_7$ secondary phases are observed for $x = 0.5$ and 1.0, respectively (Fig. 1). It should be noted here that the composition of $x = 0.5$ has been reported generally to form the single phase structure, and the appearance of $Ba_4Ti_{13}O_{30}$ secondary phase here might due to the lower calcining temperature and it is expected to vanish at a higher temperature or after sintering. Actually, there is no secondary phase is observed for the sintered ceramics with $x = 0.5$. As shown in Fig. 2, the variation of lattice parameters a, b, c and V with x indicates the obvious information on the structure change. That is, the non-monotonic variation of these parameters at $x = 0.75$ gives the evidence for the upper limit of x in $Ba_{6-3x}Nd_{8+2x}Ti_{18}O_{54}$ solid solution.

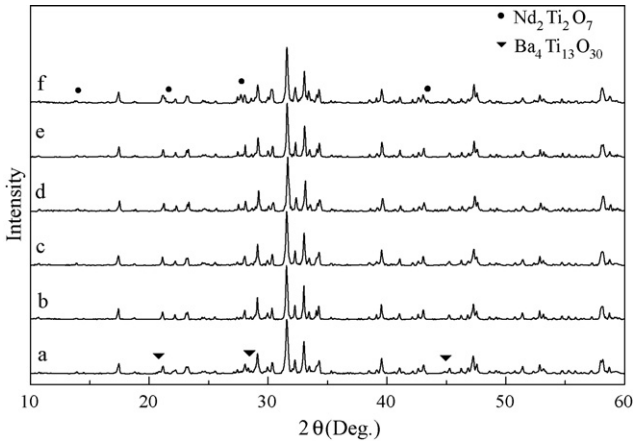

Fig. 1. XRD patterns of $Ba_{6-3x}Nd_{8+2x}Ti_{18}O_{54}$ powders calcined at 1200 °C in air for 3 h: (a) $x = 0.5$, (b) $x = 0.67$, (c) $x = 0.75$, (d) $x = 0.8$, (e) $x = 0.9$ and (f) $x = 1.0$.

Fig. 3 gives the results of high resolution XRD patterns of $Ba_{6-3x}Nd_{8+2x}Ti_{18}O_{54}$ with $x = 0.75$ and 0.8. The XRD data for $x = 0.75$ are indexed as the orthorhombic $Ba_{6-3x}Nd_{8+2x}Ti_{18}O_{54}$ tungsten bronze single phase in the space group *Pbnm*, where $a = 12.1899(4)$ Å, $b = 22.3174(7)$ Å and $c = 7.6862(2)$ Å (see Table 1). While, the situation for $x = 0.8$ is very similar, but 6.42(10) wt% of TiO_2 secondary phase is detected and the lattice parameters for the tungsten bronze phase are slightly different: $a = 12.1917(3)$ Å, $b = 22.3128(5)$ Å and $c = 7.6872(2)$ Å (Table 1). The atom positions and thermal parameter in $Ba_{3.75}Nd_{9.5}Ti_{18}O_{54}$ ($x = 0.75$) and $Ba_{3.6}Nd_{9.6}Ti_{18}O_{54}$ ($x = 0.8$) are listed in Tables 2 and 3, respectively. Fig. 4 gives the XRD patterns of the quenched samples of $Ba_{6-3x}Nd_{8+2x}Ti_{18}O_{54}$

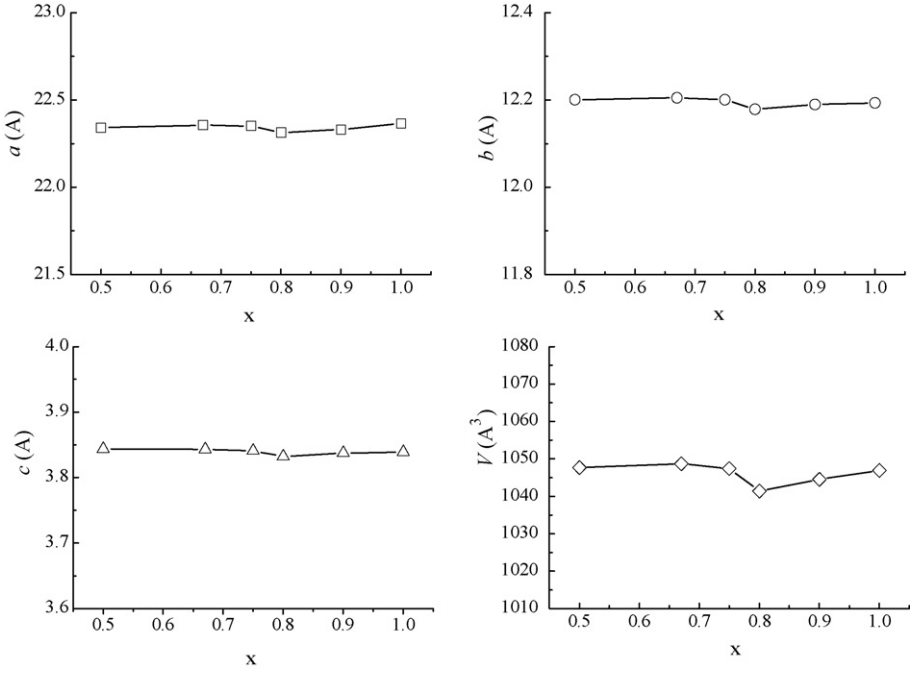

Fig. 2. Lattice parameters of $Ba_{6-3x}Nd_{8+2x}Ti_{18}O_{54}$ calcined powders as functions of x.

Table 1
Experimental parameters for X-ray powder diffraction of $Ba_{6-3x}Nd_{8+2x}Ti_{18}O_{54}$ ceramics

	$x = 0.75$	$x = 0.8$[a]
Unit cell (space group *Pbnm*, 62)	$a = 12.1899(4)$ Å $b = 22.3174(7)$ Å $c = 7.6862(2)$ Å Volume = 2091.00(11) Å^3	$a = 12.1917(3)$ Å $b = 22.3128(5)$ Å $c = 7.6872(2)$ Å Volume = 2091.16(9) Å^3
Minimum 2θ	10	10
Maximum 2θ	130	130
Total refined variables	103	103
Number of reflections	3963	3961
Profile function	Pseudo-Voigt, 0.899(7)	Pseudo-Voigt, 0.857(7)
Gaussian *U*, *V*, *W*	0.228(9), −0.096(7), 0.036(1)	0.204(9), −0.087(7), 0.037(1)
Asymmetry corrections (*P*1, *P*2)	0.057(5), 0.0354(8)	0.057(4), 0.0383(9)
Zero shift (°)	−0.069(2)	−0.065(1)
R_p (profile)	4.58	4.62
R_{wp} (weighted profile)	6.09	6.13
R_B (Bragg)	3.95	3.54
R_F	2.81	2.74
Reduced χ^2	1.77	1.81

[a] 6.42(10) wt% secondary phase TiO_2 ($P4_2/mnm$, $a = 4.5926(2)$ Å and $c = 2.9605(2)$ Å) is detected.

dense ceramics with compositions of $x = 0.75$, 0.8, 0.9 and 1.0. The tungsten bronze single phase structure is observed for $x = 0.75$, the TiO_2 secondary phase is detected for $x = 0.8$, the $Nd_4Ti_9O_{24}$ secondary phase is detected for $x = 1.0$, and both the TiO_2 and $Nd_4Ti_9O_{24}$ secondary phases are detected for $x = 0.9$. The situations for the slowly cooled samples are almost the same as those for the quenched ones. These results conclude that the stability of $Ba_{6-3x}Nd_{8+2x}Ti_{18}O_{54}$ solid solution varies

Table 2
Final atomic positions and thermal parameter of $Ba_{3.75}Nd_{9.5}Ti_{18}O_{54}$ ceramics

Atom	Wyckoff position	*x*	*y*	*z*	U_{iso} (Å^2)	Occupies
Ti_1	4a	0	0	0	0.040(3)	1.0
Ti_2	8d	0.1996(5)	0.4350(2)	−0.0111(15)	0.0157(17)	1.0
Ti_3	8d	0.3914(5)	0.1094(3)	0.0109(19)	0.042(2)	1.0
Ti_4	8d	0.1170(5)	0.1626(2)	−0.0084(15)	0.0117(16)	1.0
Ti_5	8d	0.3348(4)	0.2598(2)	−0.0128(16)	0.0210(18)	1.0
Ba_1	4c	0.0913(5)	0.30317(19)	0.25000	0.0205(13)	1.0
Ba_2	4c	0.5883(5)	0.1872(2)	0.25000	0.0279(16	0.85
Nd_1	4c	0.2013(5)	0.0498(2)	0.25000	0.0116(14)	0.819(4)
Nd_2	4c	0.7031(5)	0.4514(3)	0.25000	0.0574(19)	1.0
Nd_3	4c	1.0073(5)	0.4918(2)	0.25000	0.0232(12)	0.931(4)
Nd_4	4c	0.4006(4)	0.3796(2)	0.25000	0.0268(14)	1.0
Nd_5	4c	0.9092(4)	0.1211(2)	0.25000	0.0307(15)	1.0
O_1	4c	0.095(3)	0.1437(12)	0.25000	0.0144(13)	1.0
O_2	4c	0.558(2)	0.3100(14)	0.25000	0.0144(13)	1.0
O_3	8d	0.4064(14)	0.1964(8)	0.013(4)	0.0144(13)	1.0
O_4	8d	0.6778(12)	0.2649(7)	−0.013(4)	0.0144(13)	1.0
O_5	4c	0.314(3)	0.2877(15)	0.25000	0.0144(13)	1.0
O_6	4c	0.850(3)	0.2223(15)	0.25000	0.0144(13)	1.0
O_7	8d	0.3621(14)	0.0177(7)	0.006(5)	0.0144(13)	1.0
O_8	4c	0.234(2)	0.4509(15)	0.25000	0.0144(13)	1.0
O_9	4c	0.677(2)	0.0679(14)	0.25000	0.0144(13)	1.0
O_{10}	8d	0.2428(15)	0.1132(7)	0.053(3)	0.0144(13)	1.0
O_{11}	4c	0.504(4)	0.4798(12)	0.25000	0.0144(13)	1.0
O_{12}	8d	0.0551(16)	0.0754(8)	0.072(2)	0.0144(13)	1.0
O_{13}	8d	0.7662(13)	0.1361(7)	−0.006(5)	0.0144(13)	1.0
O_{14}	8d	0.8559(14)	0.0188(7)	0.008(6)	0.0144(13)	1.0
O_{15}	8d	0.0492(14)	0.4011(8)	0.041(3)	0.0144(13)	1.0
O_{16}	8d	0.4466(15)	0.3165(8)	0.031(3)	0.0144(13)	1.0
O_{17}	4c	0.419(3)	0.1026(13)	0.25000	0.0144(13)	1.0
O_{18}	4c	0.889(3)	0.4106(15)	0.25000	0.0144(13)	1.0

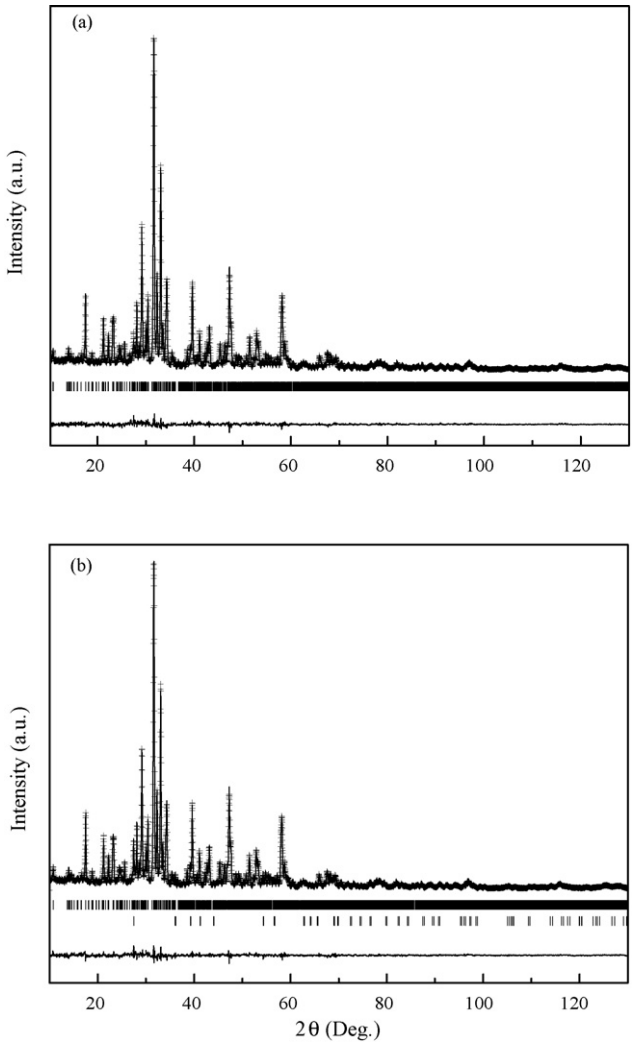

Fig. 3. High resolution X-ray powder diffraction patterns obtained at room temperature (cross) and calculated (solid line) of $Ba_{6-3x}Nd_{8+2x}Ti_{18}O_{54}$ powder. Vertical marks show the position of allowed Bragg reflections for $Ba_{6-3x}Nd_{8+2x}Ti_{18}O_{54}$ (a and b) and TiO_2 (b), respectively. A difference curve is plotted at the bottom of the pattern. (a) $x = 0.75$ and (b) $x = 0.8$.

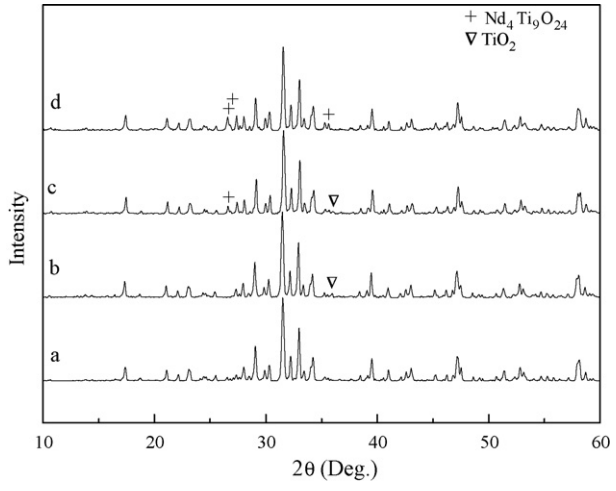

Fig. 4. XRD patterns for $Ba_{6-3x}Nd_{8+2x}Ti_{18}O_{54}$ ceramics sintered at 1350 °C in air for 3 h and quenched: (a) $x = 0.75$, (b) $x = 0.8$, (c) $x = 0.9$ and (d) $x = 1.0$.

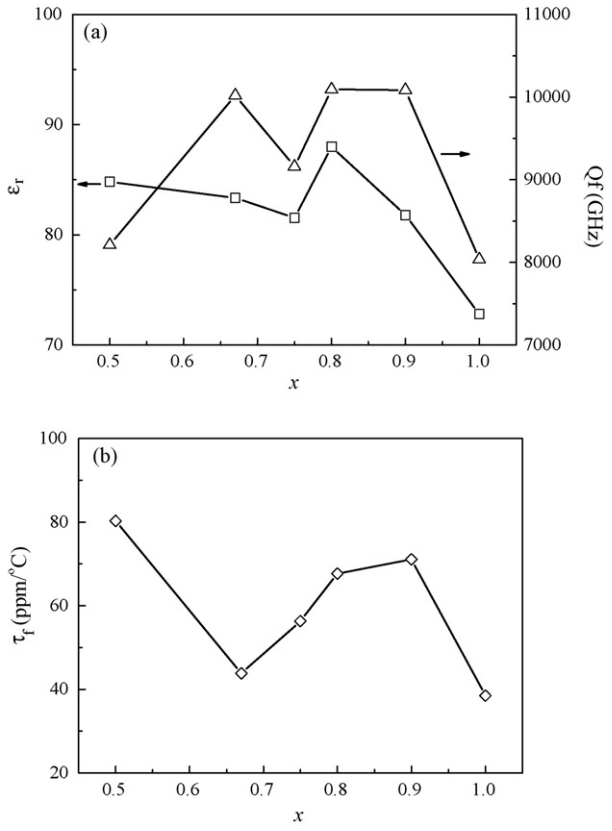

Fig. 5. Microwave dielectric characteristics of $Ba_{6-3x}Nd_{8+2x}Ti_{18}O_{54}$ ceramics sintered at 1350 °C in air for 3 h and slowly cooled at a rate of 1 °C/min: (a) ε_r and *Qf* value as functions of x and (b) τ_f as functions of x.

with x. It is the most stable at $x = 0.67$, and the stability decreases as the composition shifts from this point, and the upper limit of x is 0.75.

The microwave dielectric characteristics of $Ba_{6-3x}Nd_{8+2x}Ti_{18}O_{54}$ ceramics are shown in Fig. 5 as the functions of composition x in a wide range of 0.5–1.0. The dielectric constant varies in the range between 82 and 88 for $x = 0.5$–0.9, but a lower dielectric constant of 73 is obtained for $x = 1.0$. In addition to the maximum at 0.67 as usually reported, alternative peak of *Qf* value over 10,000 GHz is obtained at $x = 0.8$–0.9, and this value is much higher than those reported previously.[7] Moreover, a lower *Qf* value is indicated for $x = 0.75$, and this agrees with the data by Ohsato[6] and the data for as-sintered samples reported by Negas etal.[7] There is a variation tendency of τ_f with composition similar to that of dielectric constant, and the minimum values of τ_f are obtained for $x = 0.67$ and 1.0. The high *Qf* value at $x = 0.67$ can be interpreted by the lowest crystal distortion inner stress, and the high *Qf* (>10,000 GHz) value combined with high dielectric constant at $x = 0.8$–0.9 which exceed the upper limit of x is a very interesting finding, and the detailed structure origin and physical nature are worth investigating further. The possible reason for the high *Qf* value for these compositions is the release of inner stress due to the separation of secondary phases from the solid solution.

Table 3
Final atomic positions and thermal parameter of $Ba_{3.6}Nd_{9.6}Ti_{18}O_{54}$ ceramics

Atom	Wyckoff position	x	y	z	U_{iso} (Å^2)	Occupies
Ti_1	4a	0	0	0	0.031(3)	1.0
Ti_2	8d	0.2003(5)	0.4339(2)	0.0065(17)	0.0192(16)	1.0
Ti_3	8d	0.3961(5)	0.1085(2)	0.0026(16)	0.0318(17)	1.0
Ti_4	8d	0.1187(5)	0.1618(2)	−0.0039(19)	0.0327(19)	1.0
Ti_5	8d	0.3361(4)	0.2593(2)	0.0085(19)	0.0254(17)	1.0
Ba_1	4c	0.0877(5)	0.30194(19)	0.25000	0.0234(16)	0.947(7)
Ba_2	4c	0.5936(5)	0.18758(18)	0.25000	0.0128(16)	0.853(7)
Nd_1	4c	0.1999(5)	0.0486(2)	0.25000	0.0231(19)	0.894(8)
Nd_2	4c	0.7054(5)	0.4503(3)	0.25000	0.059(2)	0.992(8)
Nd_3	4c	1.0043(7)	0.4938(3)	0.25000	0.0365(13)	0.914(4)
Nd_4	4c	0.4018(6)	0.3794(2)	0.25000	0.0439(17)	1.0
Nd_5	4c	0.9060(5)	0.1210(2)	0.25000	0.0204(12)	1.0
O_1	4c	0.070(3)	0.1687(13)	0.25000	0.0151(13)	1.0
O_2	4c	0.590(3)	0.3539(12)	0.25000	0.0151(13)	1.0
O_3	8d	0.4234(14)	0.1943(9)	0.027(3)	0.0151(13)	1.0
O_4	8d	0.6763(13)	0.2638(8)	−0.028(3)	0.0151(13)	1.0
O_5	4c	0.320(3)	0.2822(17)	0.25000	0.0151(13)	1.0
O_6	4c	0.848(3)	0.2219(17)	0.25000	0.0151(13)	1.0
O_7	8d	0.3730(15)	0.0189(7)	−0.032(3)	0.0151(13)	1.0
O_8	4c	0.238(2)	0.4525(14)	0.25000	0.0151(13)	1.0
O_9	4c	0.675(2)	0.0601(14)	0.25000	0.0151(13)	1.0
O_{10}	8d	0.2571(15)	0.1135(7)	0.047(3)	0.0151(13)	1.0
O_{11}	4c	0.497(3)	0.4791(12)	0.25000	0.0151(13)	1.0
O_{12}	8d	0.0425(15)	0.0728(7)	0.042(3)	0.0151(13)	1.0
O_{13}	8d	0.7659(15)	0.1352(8)	0.046(3)	0.0151(13)	1.0
O_{14}	8d	0.8537(13)	0.0180(7)	0.014(5)	0.0151(13)	1.0
O_{15}	8d	0.0592(14)	0.4034(8)	0.044(3)	0.0151(13)	1.0
O_{16}	8d	0.4462(15)	0.3169(8)	0.020(4)	0.0151(13)	1.0
O_{17}	4c	0.427(2)	0.1030(14)	0.25000	0.0151(13)	1.0
O_{18}	4c	0.882(3)	0.4060(15)	0.25000	0.0151(13)	1.0

4. Conclusions

The upper limit of x in $Ba_{6-3x}Nd_{8+2x}Ti_{18}O_{54}$ solid solution was determined as 0.75. For compositions of $x = 0.8$, 0.9 and 1.0, the new tungsten bronze major phase was generally detected together with some secondary phases. The TiO_2 secondary phase was detected for $x = 0.8$, the $Nd_4Ti_9O_{24}$ secondary phase was detected for $x = 1.0$, and both the TiO_2 and $Nd_4Ti_9O_{24}$ secondary phases were detected for $x = 0.9$. The excellent microwave dielectric characteristics were not only obtained at $x = 0.67$ but also obtained at 0.8 and 0.9.

Acknowledgements

The present work was supported by the National Science Foundation of China under grant number 50332030, and Chinese National Key Project for Fundamental Researches under grant number 2002CB613302.

References

1. Bolton, R. L., Temperature compensating ceramics capacitors in the system baria-rare-earth-oxide titania, Ph.D. Thesis, University of Illinois, Urbana, Illinios, 1968.
2. Kolar, D., Stadler, Z., Gaberscek, S. and Suvorov, D., Ceramic and dielectric properties of selected compositions in the BaO–TiO_2–Nd_2O_3 system. *Ber. Dtsch. Keram. Ges.*, 1978, **55**, 346–347.
3. Kolar, D., Stadler, Z., Gaberscek, S., Parker, H. S. and Roth, R. S., Synthesis and crystal chemistry of $BaNd_2Ti_3O_{10}$, $BaNd_2Ti_5O_{14}$, and $Nd_4Ti_9O_{24}$. *J. Solid State Chem.*, 1981, **38**, 158–164.
4. Razogon, E. S., Gens, A. M., Varfolomeev, M. B., Korovin, S. S. and Kostomarov, V. S., The complex barium and lanthanum titanates. *Russ. J. Inorganic Chem.*, 1980, **25**(6), 945–947.
5. Matveeva, R. G., Varfolomeev, M. B. and II'yuschenko, L. S., Refinement of the composition and crystal structure of $Ba_{3.75}Pr_{9.5}Ti_{18}O_{54}$. *Russ. J. Inorg. Chem.*, 1984, **29**(1), 31–34 [in Russian].
6. Ohsato, H., Science of tungsten bronze-type like $Ba_{6-3x}R_{8+2x}Ti_{18}O_{54}$ (R = rare earth) microwave dielectric solid solutions. *J. Eur. Ceram. Soc.*, 2001, **21**, 2703–2711.
7. Negas, T. and Davies, P. K., Influence of chemistry and processing on the electrical properties of $Ba_{6-3x}Ln_{8+2x}Ti_{18}O_{54}$ solid solutions. In *Ceramic Transactions*, ed. T. Negas and H. Ling. *Materials and Processes for Wireless Communications*, *Vol 53*. The American Ceramic Society, Westerville, OH, 1995, pp. 179–196.
8. Kolar, D., Gaberscek, S., Stadler, Z. and Suvorov, D., High stability, low loss dielectrics in the system BaO–Nd_2O_3–TiO_2–Bi_2O_3. *Ferroelectrics*, 1980, **27**, 269–272.
9. Ubic, R., Reaney, I. M. and Lee, W. E., Microwave dielectric solid-solution phase in system BaO–Ln_2O_3–TiO_2 (Ln = lanthanide cation). *Intern. Mater. Rev.*, 1998, **43**(5), 205–219.
10. Gens, A. M., Varfolomeev, M. B., Kostomarov, V. S. and Korovin, S. S., Crystal-chemical and electrophysical properties of complex titanates of barium and lanthanides. *Russ. J. Inorg. Chem.*, 1981, **26**, 482–484.
11. Cruickshank, K. M., Jing, X. P., Wood, G., Lachowski, E. E. and West, A. R., Barium neodymium titanate electroceramics: phase equilibria studies of $Ba_{6-3x}Nd_{8+2x}Ti_{18}O_{54}$ solid solution. *J. Am. Ceram. Soc.*, 1996, **76**, 1605–1610.
12. Skapin, S., Kolar, D., Suvorov, D. and Samardzija, Z., Phase equilibria in the $BaTiO_3$–La_2TiO_5–TiO_2 system. *J. Mater. Res.*, 1998, **13**(5), 1327–1334.

13. Belous, A. G., Ovchar, O. V., Valant, M., Suvorov, D. and Kolar, D., The effect of partial isovalent substitution in the A-sublattice on MW properties of materials based on $Ba_{6-3x}Ln_{8+2x}Ti_{18}O_{54}$ solid solutions. *J. Eur. Ceram. Soc.*, 2001, **21**, 2723–2730.
14. Wu, Y. J. and Chen, X. M., Modified $Ba_{6-3x}Nd_{8+2x}Ti_{18}O_{54}$ microwave dielectric ceramics. *J. Eur. Ceram. Soc.*, 1999, **19**, 1123–1126.
15. Wu, Y. J. and Chen, X. M., Bi/Sm co-substituted $Ba_{6-3x}Nd_{8+2x}Ti_{18}O_{54}$ microwave dielectric ceramics. *J. Am. Ceram. Soc.*, 2000, **83**, 1837–1839.
16. Wu, Y. J. and Chen, X. M., Structures and microwave dielectric properties of $Ba_{6-3x}(Nd,Bi)_{8+2x}Ti_{18}O_{54}$ ($x = 2/3$) solid solution. *J. Mater. Res.*, 2001, **16**, 1734–1738.
17. Chen, X. M. and Li, Y., A- and B site cosubstituted $Ba_{6-3x}Sm_{8+2x}Ti_{18}O_{54}$ microwave dielectric ceramics. *J. Am. Ceram. Soc.*, 2002, **85**(3), 570–584.
18. Li, Y. and Chen, X. M., Effects of sintering conditions on microstructures and microwave dielectric properties of $Ba_{6-3x}(Sm_{1-y}Nd_y)_{8+2x}Ti_{18}O_{54}$ ceramics ($x = 2/3$). *J. Eur. Ceram. Soc.*, 2002, **22**, 715–719.
19. Chen, X. M., Qin, N. and Li, Y., Microstructure and microwave dielectric characteristics of $Ba_{6-3x}(Sm_{1-y}La_y)_{8+2x}Ti_{18}O_{54}$ Solid Solutions ($x = 2/3$ and 0.75). *J. Electroceram.*, 2002, **9**(1), 31–35.
20. Wu, S. Y., Li, Y. and Chen, X. M., Raman spectra of $Ba_{6-3x}Sm_{8+2x}Ti_{18}O_{54}$ solid solution. *J. Phys. Chem. Solids*, 2003, **64**, 2365–2368.
21. Li, Y., Chen, X. M., Qin, N. and Zeng, Y. W., Tin substitution for titanium in $Ba_{6-3x}Nd_{8+2x}Ti_{18}O_{54}$ microwave dielectric ceramics. *J. Am. Ceram. Soc.*, 2005, **88**(2), 481–484.
22. Qin, N., Chen, X. M. and Liu, X. Q., Dielectric anomaly and phase transition in $Ba_{6-3x}(Sm_{1-y}La_y)_{6+2x}Ti_{18}O_{54}$ ($x = 0.5$) ceramics. *J. Am. Ceram. Soc.*, 2006, **89**(9), 2796–2803.
23. Rodríguez-Carvajal, J., Recent developments of the program FULLPROF, in commission on powder diffraction (IUCr). *Newsletter*, 2001, **26**, 12–19.
24. Hakki, B. W. and Coleman, P. D., A dielectric resonator method of measuring inductive capacitance in the millimeter range. *IRE Trans. Microwave Theory Tech.*, 1960, **8**, 402–410.